

RCS Measurement and Analysis of Rectangular and Circular Cross-section Cavities

Abhinav Bharat, M L Meena, S. Sunil Kumar, Neha Sangwa, Shyam Rankawat
Defence Laboratory, DRDO
Jodhpur, India-342011

Abstract— The RCS of re-entrant structures, like cavities, is difficult to estimate either using High-Frequency Computational Electromagnetics (CEM) solvers with multi-bounce capability, or with exact solvers. Results from High-Frequency solvers are not consistent amongst themselves, or with measured data. Exact solvers, such as MoM, require heavy compute resources, and cavity structures make the convergence slower.

In this work, the RCS of a simple circular cross-section duct and a simple rectangular cross-section duct has been investigated using both computations and measurements. The ducts have been fabricated and embedded into a low-RCS testbody, so that only the duct-contributions are measured. The results of the measurements, carried out at DRDO's NFDRE RCS Range, are presented. The RCS of the ducts were computed using an SBR Solver, and using an MoM solver. The measured data is compared with the results of the computations. It is shown that the High-Frequency Solver is inadequate to correctly predict the RCS behavior of ducts, even for very simple duct shapes.

Keywords- RCS, SBR, MOM

I. INTRODUCTION

In real-world electromagnetic problems, like scattering, radiation, etc. for electrically large objects with cavity are not analytically calculable. Cavity structures, such as air-intakes and exhausts of an aircraft, give rise to large backscatter echo over a wide angular sector, and therefore, require critical attention in the design of low-observable platforms. The measurement of radar echo from real target is costly and complex equipments are involved in measurement setup. For such setup, precise positioning of antennas, fairly clean (low background clutter and multipath) measurement facility including LO pylon, and accurate angular scan become mandatory. In addition, the microwave instrumentation should be configured to illuminate the object with sufficient energy so that the returned signal from test target has sufficient isolation w.r.t., the background clutter.

The measurement of complex cavity shapes further requires a suitable setup such that only the interior portion of cavity is irradiated with Electromagnetic interaction. So, it becomes necessary to hide the cavity outer surface from EM interaction. This can be performed either by appropriate placement of absorbers around the cavity periphery or by blending the cavity structure on a low RCS testbody, e.g., Almond testbody. Thus, an accurate characterization of the complex cavity structures radar scattering is a rather challenging task.

CEM solvers have been in use for modeling the interaction of electromagnetic fields with physical objects and related scattering. Several numerical techniques are present which can derive the results by solving the closed form of Maxwell's equations. An effort into analysis of cavity shapes has been taken up by applying various numerical techniques for such analysis. The techniques though very well suited for single bounce analysis have been put to test for the multi-bounce phenomenon involved in our scenario.

This paper presents the monostatic RCS study in azimuth plane for Rectangular and Circular cross-section cavities. Both the computational and measurement techniques have been used for RCS analysis, exclusively at an incident frequency of 10GHz. The computation results have been generated for the study performed using a High Frequency solver (PO-PTD), a full-wave solver (MLFMM) and through Near-field RCS measurements.

II. SIMULATION AND MEASUREMENT TECHNIQUES UTILIZED

The solution to the Electromagnetic scattering problems requires an appropriate solution of the Maxwell's Equations. For the computational techniques involving surface meshes, the surface of the object is discretized into small elements (triangles or quadrilaterals). This mesh is then utilized for the computation of induced Electric and Magnetic fields (or

induced charges and currents) w.r.t. the incident Electromagnetic waves along with application of suitable boundary conditions at the interfaces. Here, we have used two solvers, (i) Asymptotic solver based on PO-PTD with multi-bounce capability, (ii) Full-wave solver based on MLFMM technique.

Asymptotic Solver (PO-PTD with multi-bounce):

The Asymptotic computation technique is an analysis in the frequency domain based on use of different high frequency approximation methods like GO, GO-GTD, PO, PO-PTD, hybrid SBR. The incident and reflected rays can be considered either independent or bundled together within the ray tubes. This solver is typically used for scattering computations on electrically very large objects which are difficult to handle by other EM solution methods. The mesh generation is very robust and quite insensitive to the quality of the CAD model.

The approximation involved is the use of ray optics approach to estimate the induced surface currents and hence, to calculate the scattered fields.

Full-wave Solver (MLFMM/ MoM): The full-wave solver based on integral equation solution to Maxwell's Equations, is of special interest for electrically large objects. Here, the discretization of the calculation domain is reduced to the object boundaries (surface mesh), which leads to the solution of a linear equation system with less unknowns than the volumetric techniques. The integral equation solver based on MoM technique creates a dense matrix, as each element is considered coupled to all other discretized elements of the object. The other technique, Fast Multipole Method (FMM), further uses the sub-division of computation domain to boxes so as to combine the corresponding coupling sparse matrices. Another technique, Multi-Level Fast Multipole Method (MLFMM), further uses a recursive sub-division scheme to speed up this matrix vector multiplication process.

So, the MLFMM solver is more suitable for analysis of very large electrical size problems as the standard MoM approach becomes cumbersome. It speeds up the matrix vector multiplications, which are dominating operations in the iterative solver and also enhances the memory efficiency of computation platform. The solver time for MLFMM is estimated as $N_{iter} \cdot N \cdot \log(N)$ while for MoM it is approximately N^3 . Similarly, the memory requirement for MLFMM is approximately $N \cdot \log(N)$ as compared to N^2 for MoM.

Measurement Method: EM waves are transmitted towards the target and the received signal can be used to determine the shape and composition of target. SAR and ISAR techniques are used for collection of this

backscattered echo. In our case, at NFDRF range, DRALA complex, DL Jodhpur, ISAR technique has been employed for RCS data acquisition through measurements. In ISAR technique, the target to be analyzed is rotated over the angular sector of interest while the radar is kept stationary. The reflectivity data is collected at each angular sample over the whole frequency band. The target of interest can be considered as comprising of various reflecting centers called scatterers and the total backscattered echo at the receiver T_{field} is the vector (phase and magnitude) sum of the reflectivity data received from these scatterers:

$$T_{field} = \kappa \iint_{area} \rho(x, y) \exp\left(\frac{-j2\pi(2d(x, y))}{\lambda}\right) dx dy \quad (3)$$

where,

κ = a proportionality constant,

$\rho(x, y)$ = 2D spatial distribution of reflectivity,

$d(x, y)$ = distance of reflecting centre to antenna aperture,

λ = wavelength of incident wave,

The total field thus depends on the wavelength of incident wave, reflectivity of point scatterers and the distance between observation point and the point scatterer. This field data at the receiver is then calibrated to estimate the expected RCS levels.

III. TESTBED AND CAVITY SHAPES

An Almond shape (low RCS body) [1] of length 125cm was designed and developed as a testbed for performing RCS computation and measurement studies on rectangular and circular cross-section cavities as shown in Figure 1. This testbed was identified as having very low signature in the frontal sector and selected for performing measurements of backscatter echo from the interior of the cavities, while removing scattering from its exterior surface. The only source of backscatter, that was observed from the testbed (within X-Band), is the tip-diffraction effect from its nose.



Figure 1 Fabricated Almond-shaped testbed

The open ended rectangular and circular cross-section cavities (dimensions described in Figure 2 &

Figure 3, respectively) were then blended on to the low RCS testbed (Figure 4 & Figure 5). The cavities are placed inside the almond testbed with their axis placed horizontally w.r.t. the ground. The cavity openings were also blended with the surface of almond testbed. The fabrication of the measurement models was done using FRP, the surface of which was subsequently metallized using conductive paint coating.

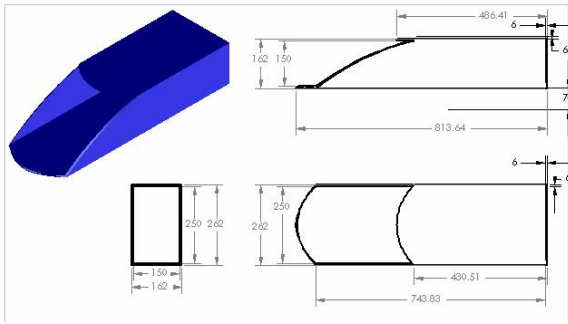


Figure 2 The dimension of the rectangular cross section is 15 cm x 25 cm. The cavity lower and upper faces length is about 74 cm and 43 cm. These lengths are chosen so as to fit in a 125 cm almond shaped testbed

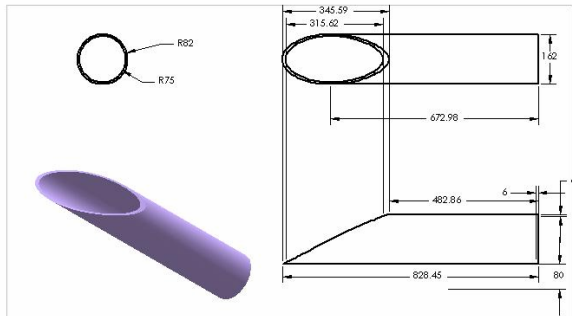


Figure 3 The diameter is 150 cm. The maximum length is about 83 cm and minimum length is about 49 cm

RCS analysis of the models was carried out at X-Band (10 GHz) by means of both computations and measurements. At this frequency, the electrical size of the rectangular cavity aperture (distance between parallel plates) for azimuth plane scan is approximately 10λ . So, the ray bouncing approach is expected to yield adequate similarity to the full-wave solver results for this high frequency analysis. But, the diameter of circular cross-section cavity aperture is approximately 5λ . So, ray optical behavior assumption may not be suitable for analysis of this cavity shape, as suggested by the available literature.

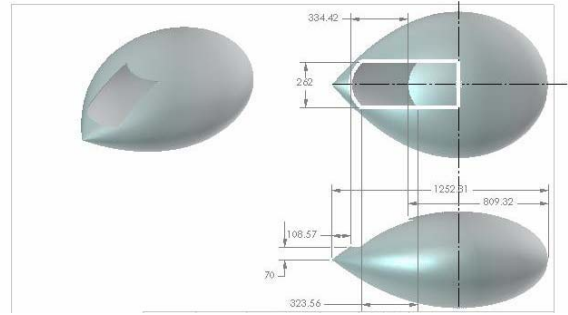


Figure 4 Rectangular cavity blended in low-RCS testbed

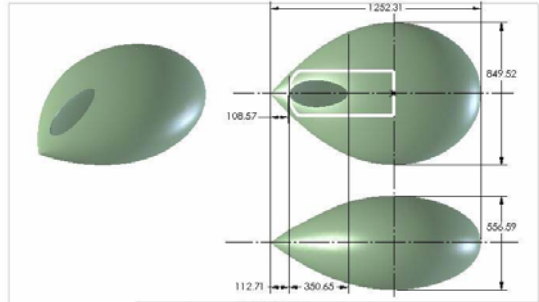


Figure 5 Cylindrical cavity blended in low-RCS testbed

IV. TESTBED VERIFICATION

A verification study of the blending of rectangular and circular cross-section cavities within the low-RCS Almond testbed is as shown in Figure 6. The plot shows measured RCS levels vs. aspect angle in azimuth plane at 10 GHz incident frequency, horizontal polarization, for almond testbed and almond with rectangular & circular cross-section cavities. This plot clearly suggests that the RCS levels of almond shaped testbed is quite low (below -20 dBsm) in the angular window of Nose-on ± 40 deg. So the cavity shapes can be blended on such platform for RCS analysis within this angular window.

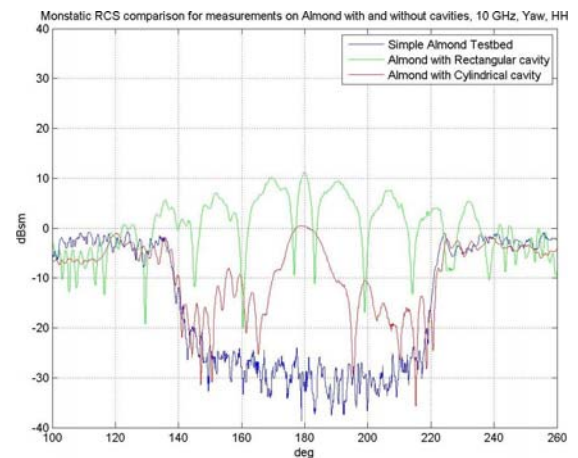


Figure 6 RCS plot of Almond testbed and blending with Rectangular and Cylindrical Cavity- Measured results, 10 GHz, azimuth plane, horizontal polarization

V. RESULTS & OBSERVATIONS

A comprehensive study was performed to analyze the RCS response as a function of aspect angle in azimuth plane for three models: (i) simple almond shaped testbed of length 125cm, (ii) rectangular cross-section cavity blended on the almond shaped testbed, (iii) circular cross-section cavity blended on the almond shaped testbed. The study shown here, is mainly focused on analysis of the scattering response at 10 GHz and horizontal polarization. Data was collected from computations carried out using commercially available Asymptotic solver and MLFMM solver and also through measurements at NFDRF range.

The results of analysis of low RCS testbed, rectangular and circular cross-section cavity blended on testbed using different solvers and measurements are shown in Figure 7, Figure 8 and Figure 9, respectively.

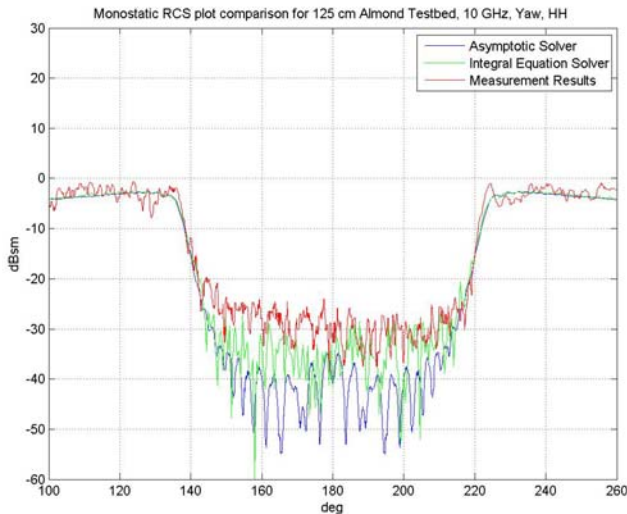


Figure 7 RCS comparison plot of Almond shaped testbed for Asymptotic, Integral Equation(MLFMM) solver and measurement results, 10 GHz, azimuth plane, horizontal polarization

As observed in Figure 7, a low-RCS angular window is observed for the almond shape testbed within Nose-on ± 40 deg span for all the results. The measured results are observed to be slightly higher as compared to the computation results. The computation results from the full-wave solver are more closer to the measurement results. This difference in the RCS levels can be attributed due to: (i) dominant tip diffraction effects in the testbed within the low-RCS angular window, (ii) approximate nature of the Asymptotic solver, (iii) manufacturing deformities.

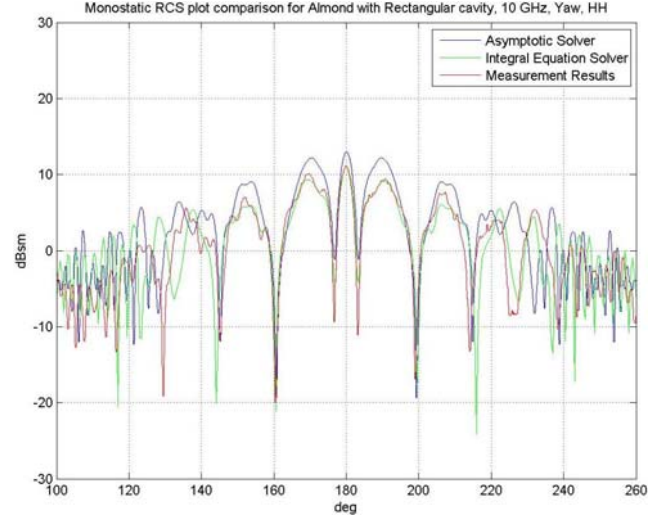


Figure 8 RCS comparison plot of rectangular cross-section cavity blended on Almond shaped testbed for Asymptotic, Integral Equation(MLFMM) solver and measurement results, 10 GHz, azimuth plane, horizontal polarization

Figure 8 shows similar RCS comparison results for rectangular cross-section cavity blended on almond shaped testbed. For Nose-on incidence, if only the flat plate present at the cavity backing is assumed dominant, then the observed RCS level should be about +12.93 dBsm. However, such Nose-on incidence RCS level is observed only for computation results of Asymptotic solver. The results for full-wave solver computations and measurements are slightly lower in magnitude and have good correlation between them. This reflects the approximate nature of Asymptotic solver, whose accuracy decreases with the decrease in electrical size of the cavity aperture. However, considering the good correlation observed with other results, the solver can still be used as a time efficient alternative.

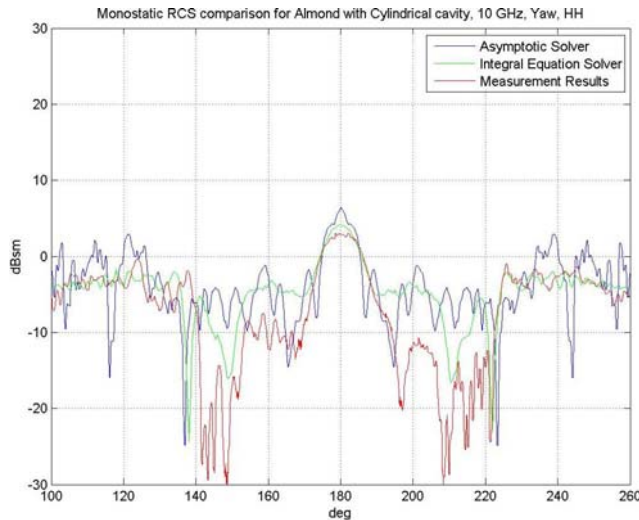


Figure 9 RCS comparison plot of circular cross-section cavity blended on Almond shaped testbed for Asymptotic, Integral Equation(MLFMM) solver and measurement results, 10 GHz, azimuth plane, horizontal polarization

Similarly, Figure 9 shows the RCS comparison plots for circular cross-section cavity blended on almond shaped testbed. For Nose-on incidence, if only the flat plate present at the cavity backing is assumed dominant, then the observed RCS level in this case should be about +6.40 dBsm. However, only the Asymptotic solver is seen to show such Nose-on incidence RCS level. The results for full-wave solver computations and measurements are slightly lower in magnitude and have better correlation between them as compared to the Asymptotic solver. This RCS plot demonstrates the effect of reduction in RCS levels due to partial blocking of Electromagnetic waves at the cavity aperture. The asymptotic solver is seen not able to properly capture the RCS response over the angular sector. The full-wave solver is although observed more close to the measurement results. However, slight deviations are expected from measurement results possibly due to inaccurate positioning of the almond as well as cavity back-plate in both pitch and tilt aspects.

VI. CONCLUSIONS

The cavity structures are observed as prime back-scatterers on aircraft platforms while present as air-intakes and exhaust cavities. They show a significant increase in the observed RCS levels over a wide angle sector both in azimuth and pitch planes when blended on such platforms.

In order to assess the RCS contribution of typical cavity shapes due to interior irradiation with Electromagnetic waves while ignoring the contribution from its outer surface, the cavity shapes were blended on a specially designed models of low-RCS testbed, which were also subsequently fabricated.

The RCS study was then performed on these models by means of both measurements and computational tools: both approximate and exact solvers.

The observations are as mentioned below:

- i. The low-RCS almond testbed can be used to study the cavity RCS within the Nose-on ± 40 deg angular sector in azimuth plane
- ii. The full-wave solver simulations should obviously be the choice for cavity RCS estimation however, owing to multi-bounce phenomenon involved, they show lesser rate of convergence and hence are not time efficient.
- iii. For the cavity aperture diameter exceeding 10λ size, the asymptotic solver is expected to give good correlation with the actual results. So they can be preferred for analysis of electrically very large cavity apertures as they are time efficient.
- iv. The positioning of the almond shaped testbed is very crucial for both pitch and tilt aspects in order to correctly predict the RCS of blended cavity shape.

ACKNOWLEDGEMENTS

The authors would like to acknowledge ADA, Bangalore team for their support to this activity. The support received from Director, DLJ, Dr SR Vadera, and the kind guidance received from Group Head, Ms Anjali Bhatia, is acknowledged. We further extend our sincere gratitude to the support staff at NFDRF Range, DL Jodhpur.

REFERENCES

1. 'US Patent No. 4809003 for Almond Test Body', *Dominek et al, dated 28 Feb 1989*
2. 'High Frequency RCS of Open Cavities with Rectangular and Circular Cross Sections', *Ling, Lee, Chou, IEEE Trans. AP-37, May 1989*
3. 'Shooting and Bouncing Rays: Calculating the RCS of an Arbitrarily Shaped Cavity', *Hao Ling, Ri Chee Chou, Shung Wu Lee, IEEE Trans. AP-37, Feb 1989*
4. 'RCS Study of Air Intake Configuration of AURA' *Interim Technical Progress Report, Defence Lab Jodhpur, Feb 2012*